Role of Coulomb repulsion in correlated-electron emission from a doubly excited state in nonsequential double ionization of molecules

Cheng Huang,[1,*] Wenliang Guo,[1] Yueming Zhou,[2] and Zhengmao Wu[1]
[1]*School of Physical Science and Technology, Southwest University, Chongqing 400715, China*
[2]*School of Physics, Huazhong University of Science and Technology, Wuhan 430074, China*
(Received 9 August 2015; published 19 January 2016)

With the classical ensemble model, we investigate nonsequential double ionization of aligned molecules by few-cycle laser pulses at low intensity, where the two electrons finally are ionized through a transition doubly excited state induced by recollision. The correlated electron momentum distribution of parallel molecules exhibits the line-shaped structure parallel to the diagonal. Our analysis indicates that besides the ionization time difference of two electrons from the doubly excited state, the final-state *e-e* Coulomb repulsion plays a vital role in the formation of the line-shaped structural momentum distribution. For perpendicular molecules, due to the prominent near half-cycle ionization time difference between the two electrons from the doubly excited state, the momentum distribution shows clear anticorrelation behavior.

DOI: 10.1103/PhysRevA.93.013416

I. INTRODUCTION

Nonsequential double ionization (NSDI) is one of the most fundamental and attractive phenomena in the strong-field physics field because it involves the correlated motion of two electrons [1–4]. Different from sequential double ionization (SDI) where the two electrons are ejected one by one independently [5–7], NSDI proceeds by a recollision process [8,9]. There, the first released electron is driven back by the oscillating laser field and collides with the parent ion inelastically, leading to the second electron being released. The ionization dynamics of the two electrons after recollision depends strongly on the laser intensity. At high intensity, the return electron obtains a large amount of energy from the laser field. Thus it can directly knock out the second electron when it recollides with the parent ion, which is called direct recollision ionization. At moderate intensity, the energy of the return electron is not enough to directly knock out the other one, but by recollision it can excite the second electron and keep free itself. Subsequently the excited electron is ionized by the laser electric field [10]. At lower laser intensity, after recollision, the recolliding electron gets recaptured and forms a transition doubly excited state, and then the two electrons are released from the doubly excited state [11].

In the study of NSDI, the correlated-electron momentum spectrum has been the most powerful tool for unveiling the ultrafast dynamics of correlated two electrons [12–17]. Many novel characteristics have been found in the correlated electron momentum spectra [18–22] and helped reveal many detailed microscopic dynamics processes in NSDI. For example, the fingerlike (or V-like) structure [18,19] in the correlated-electron momentum spectrum of helium indicates the roles of the nuclear attraction at recollision and final-state *e-e* repulsion at relatively low intensity [23,24] and reveals asymmetric energy sharing during recollision at the high intensity [25]. At intensities below the recollision threshold, the anticorrelated momentum spectrum from NSDI of Ar atoms [22] implies the delayed emission of the second electron after recollision [26].

The correlated-electron momentum spectra above have been measured using many-cycle laser pulses, where the contribution of multiple recollisions to NSDI could hamper further understanding of the detailed recollision dynamics. Because the few-cycle laser pulse can achieve only one single recollision event, NSDI driven by few-cycle laser pulses receives increasing attention [27–31]. Recently, Bergues *et al.* completed the measurement of correlated-electron momentum spectra for NSDI of Ar atom and N_2 by few-cycle laser pulses at high intensity (3×10^{14} W/cm^2) [32,33]. The correlated-electron momentum spectra exhibit a cross-shaped structure that qualitatively differs from spectra recorded using many-cycle pulses. Almost at the same time the correlated-electron momentum spectra for NSDI of Ar atom by few-cycle laser pulses at low intensity (9×10^{13} W/cm^2) were measured by Camus *et al.*, which show a line-shaped structure parallel to the diagonal. It is attributed to the ionization time difference of two electrons from the doubly excited state. Since at high intensity the correlated-electron momentum spectra of atoms and molecules by few-cycle pulses both exhibit the same cross-shaped structure. At low intensity, does the correlated-electron momentum spectra of molecules by few-cycle laser pulses exhibit the same line-shaped structure as that of atoms? Furthermore, from Fig. 2 of Ref. [34] one can see that large numbers of NSDI events have near-zero ionization time differences, for which the final-state *e-e* Coulomb repulsion can accelerate an electron and block the other electron, forming a momentum difference between two electrons. Thus it can be expected that final-state *e-e* repulsion should play a important role in the formation of the line-shaped structure. What extent is the line-shaped structure affected by the final-state *e-e* repulsion? It is not discussed in Ref. [34]. Additionally, the previous study using the many-cycle laser pulse has demonstrated that correlated-electron dynamics is significantly affected by the molecular alignment [35]. What is the situation for NSDI of different aligned molecules by few-cycle laser pulses at low intensity? These questions are what we want to address here.

In this paper, we investigate NSDI of aligned molecules by few-cycle laser pulses at low intensity. Our study indicates that the same as for atoms, the NSDI of aligned molecules by few-cycle pulses at low intensity occurs through a transition doubly

*huangcheng@swu.edu.cn

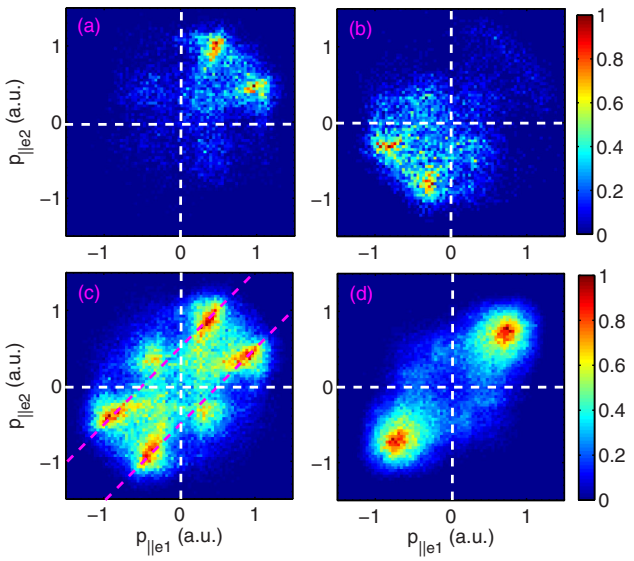

FIG. 1. Correlated-electron momentum distributions for NSDI of molecules aligned parallel to the laser polarization by 800 nm, four-cycle linearly polarized laser pulses at the intensity of 1×10^{14} W/cm^2. (a) ϕ=0, (b) $\phi = 0.5\pi$, (c) all CEPs averaged, (d) all CEPs averaged but the final-state *e-e* repulsion is neglected by replacing the long-range Coulomb repulsion with the short-range Yukawa potential (see the text for details). The ensemble size is 3×10^7 in (a) and (b), 3×10^8 in (c) and (d).

excited state induced by recollision. The correlated-electron momentum distribution of parallel molecules exhibits a line-shaped structure parallel to the diagonal. The comparison between those calculations including and excluding final-state *e-e* repulsion demonstrates that the final-state *e-e* repulsion plays a vital role in the formation of the line-shaped structural momentum distribution. However, the correlated momentum distributions of perpendicular molecules by few-cycle laser pulses at low intensity do not show the line-shaped structure but the anticorrelation behavior. It is attributed to prominent near half-cycle emission delay between two electrons from the doubly excited state.

II. CLASSICAL ENSEMBLE MODEL

In the past decade, numerous studies have convincingly confirmed that the classical ensemble model is a reliable tool in exploring electron dynamics in strong-field NSDI [36–39]. It succeeded not only in explaining the experimental data but also predicting new phenomena [13,15]. Note that in the classical model the electrons are ionized over the suppressed barrier and no tunneling ionization occurs. Thus the classical model can only obtain the qualitative result and cannot describe the strong-field processes at the quantitative level. Very recently, Camus *et al.* [34] employed the classical model to reproduce well the line-shaped structure in electron momentum spectra from NSDI by the few-cycle laser pulse at low intensity. Existence of the doubly excited state has been confirmed. In this paper, we explore mainly the role of the final-state *e-e* Coulomb repulsion on ionization dynamics of the two electrons from the doubly excited state with the classical three-dimensional ensemble model.

In this classical ensemble model, the evolution of the molecular system is determined by Newton's equations of motion (atomic units are used throughout unless stated otherwise):

$$\frac{d^2\mathbf{r}_i}{dt^2} = -\nabla[V_{ne}(\mathbf{r}_i) + V_{ee}(\mathbf{r}_1,\mathbf{r}_2)] - \mathbf{E}(t), \qquad (1)$$

where the subscript i is the label of the two electrons. $\mathbf{r}_i$ represent the electronic coordinates, and $\mathbf{R}$ is the internuclear distance vector. In the present calculations, the internuclear distance R is set to be 2.0 a.u. $\mathbf{E}(t)$ is the electric field of an 800 nm linearly polarized laser pulse with a four-cycle $\sin^2$-shaped envelope at the intensity of 1×10^{14} W/cm^2. It is written as $\mathbf{E}(t) = \hat{\mathbf{e}}_\mathbf{z} E_0 \sin(\pi t/\tau)^2 \cos(\omega t + \phi)$. Where $\hat{\mathbf{e}}_\mathbf{z}$ is the polarization vector. E_0, ω, ϕ, and τ are the electric field amplitude, angular frequency, the carrier-envelope phase (CEP), and the total duration of the pulse, respectively. The potentials $V_{ne}(\mathbf{r}_i) = -1/\sqrt{(\mathbf{r}_i + \mathbf{R}/2)^2 + a} - 1/\sqrt{(\mathbf{r}_i - \mathbf{R}/2)^2 + a}$ and $V_{ee}(\mathbf{r}_1,\mathbf{r}_2) = 1/\sqrt{(\mathbf{r}_1 - \mathbf{r}_2)^2 + b}$ represent the electron-nuclear and electron-electron interactions, respectively. To avoid autoionization, we set the screening parameter a to be 1.25; b is set to be 0.0025. To obtain the initial values, the ensemble is populated starting from a classically allowed position for the H_2 ground-state energy of -1.67 a.u. The available kinetic energy is distributed between the two electrons randomly in momentum space. Then the electrons are allowed to evolve a sufficiently long time (400 a.u.) in the absence of the laser field to obtain stable position and momentum distribution. Once the initial ensemble is obtained, the laser field is turned on and all trajectories are evolved in the combined Coulomb and laser fields.

III. RESULTS AND DISCUSSION

Figures 1(a) and 1(b) show the CEP-resolved correlated-electron momentum distributions for NSDI of molecules aligned parallel to the laser polarization for CEPs ϕ=0 and $\phi = 0.5\pi$, respectively. One can see that these NSDI events are mainly clustered in the first or third quadrants, i.e., the two electrons prefer to escape away from the parent ion into the same hemisphere. The asymmetry of those NSDI events emitted into the first and third quadrants has been well understood by means of the asymmetry of the electric field of the few-cycle laser pulse [27,28]. Figure 1(c) displays CEP-averaged correlated-electron momentum distribution for NSDI of parallel molecules. Different from the case of many-cycle pulses, where NSDI events mainly distribute around the diagonal [35], here most of NSDI events distribute along two distinct lines being parallel to the diagonal which is similar to that of atoms driven by few-cycle laser pulses at low intensity [34]. The line-shaped structure indicates that there exists a momentum difference between two electrons from NSDI.

To explore the origin of the line-shaped structure in the correlated-electron momentum distribution, we trace classical NSDI trajectories and carefully back examine their histories. In this way, we can easily obtain the recollision time and final ionization times of two electrons. Here, the recollision time is defined to be the instant of the closest approach after the first departure of one electron from the parent ion. We

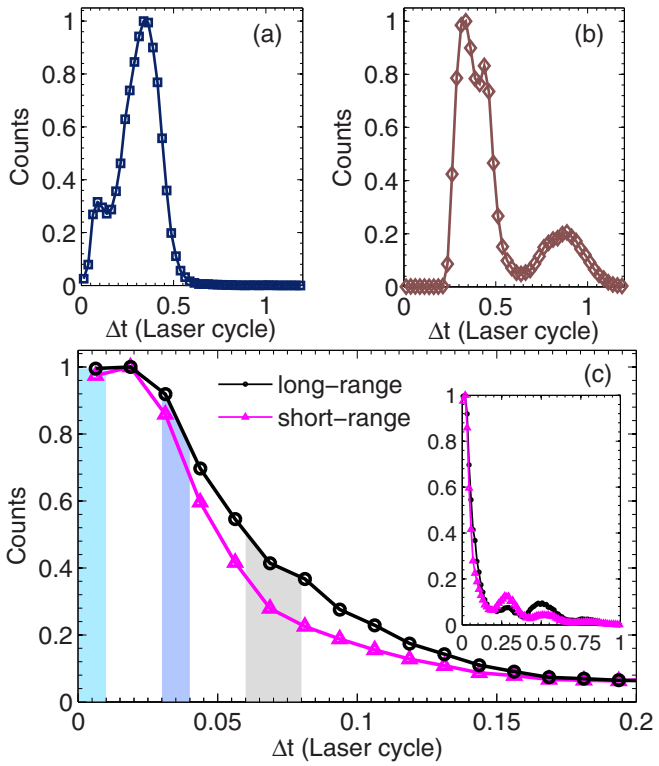

FIG. 2. Distributions of time delay between final ionizations of the two electrons and the recollision: (a) the first electron, (b) the second electron. The two electrons are numbered based on the final ionization order from the doubly excited state. (c) Distribution of ionization time difference of two electrons from the doubly excited state. Black curve: long-range potential for *e-e* interaction; magenta curve: short-range Yukawa potential for *e-e* interaction. The inset shows a larger range.

define an electron to be ionized if its energy turns positive, where the energy of each electron contains the kinetic energy, potential energy of the electron-ion interaction, and half electron-electron repulsion. In the present work, because of the low laser intensity and the small energy of the return electron, after recollision the return electron gets recaptured and forms a transition doubly excited state, and then the two electrons are ionized by the laser field from the doubly excited state. Based on the final ionization order from the doubly excited state the two electrons are defined as the first and the second electron. Both electrons are mainly ionized later than 0.3 laser cycle after recollision, as shown in Figs. 2(a) and 2(b).

Because the intermediate doubly excited state has lost memory of its formation dynamics [34], we only need analyze the emission dynamics of the two electrons from the doubly excited state. The black curve of Fig. 2(c) shows the distribution of the ionization time difference of the two electrons from the doubly excited state. The distribution of the ionization time difference has a peak around $\Delta t = 0$ and then decreases rapidly with the time difference increasing, which is very similar to the case of an atom (see Fig. 2 of Ref. [34] which is obtained by the doubly exited complex calculation). In Ref. [34], the line-shaped structure of atoms is attributed to the ionization time difference of two electrons from the transition doubly excited state. However, one can see large numbers of NSDI events have near-zero ionization time difference of two electrons. For the two electrons from these NSDI events the acceleration of the laser electric field almost is the same and cannot result in the final momentum difference. On the other hand, when two electrons almost ionize at the same time, the Coulomb repulsion between two electrons is quite strong and can prominently accelerate an electron and block the other electron, finally forming a momentum difference between the two electrons. Because a peak at zero point in the distribution of the ionization time difference appears [see the black curve of Fig. 2(c)], it can be expected that final-state *e-e* repulsion plays an important role in the formation of the line-shaped structure. In the following, we will try our best to clarify the role of final-state *e-e* repulsion in the formation of the line-shaped structure in the correlated-electron momentum of parallel molecules.

As discussed above, it is expected that final-state *e-e* repulsion can result in prominent momentum difference for those NSDI events with near-zero ionization time differences. To identify the role of the final-state *e-e* repulsion in forming the line-shaped structure of the correlated-electron momentum distribution, we have performed an additional calculation, in which once one electron is ionized from the doubly excited state, the final-state *e-e* interaction $V_{ee}(\mathbf{r}_1,\mathbf{r}_2) = 1/\sqrt{(\mathbf{r}_1-\mathbf{r}_2)^2+b}$ is replaced by the short-range Yukawa potential $V_{ee}(\mathbf{r}_1,\mathbf{r}_2) = \exp[-\kappa r_b]/r_b$, where $r_b = \sqrt{(\mathbf{r}_1-\mathbf{r}_2)^2+b}$ and $\kappa = 5.0$ [24,25]. In this way, we obtain the result where the final-state *e-e* repulsion is neglected. The corresponding correlated-electron momentum distribution is shown in Fig. 1(d). The NSDI events mainly cluster at the diagonal in the first and the third quadrants and the line-shaped structure disappears. Thus this result confirms that the final-state *e-e* Coulomb repulsion plays a decisive role in the formation of the line-shaped structure in correlated-electron momentum distribution.

The magenta curve of Fig. 2(c) shows the distribution of the ionization time difference of the two electrons from the doubly excited state for the case excluding the final-state *e-e* repulsion. The distribution is similar to that with final-state *e-e* repulsion considered. The ionization time differences of the two electrons of most NSDI events are smaller than $0.2T$. To identify the relative contribution of the final-state *e-e* repulsion and ionization time difference of the two electrons on final electron momentum difference, we carefully analyze those NSDI events from three different ionization time differences. They are $[0T,0.01T]$, $[0.03T,0.04T]$, and $[0.06T,0.08T]$, which are also marked with shadows in Fig. 2(c). The first and second rows of Fig. 2 display the correlated-electron momentum distributions for the cases including and excluding the final-state *e-e* repulsion, respectively. Each column from left to right corresponds to the ionization time difference of $[0T,0.01T]$, $[0.03T,0.04T]$, and $[0.06T,0.08T]$, respectively. Those plots in the third row show the distributions of longitudinal momentum difference $\Delta p_{||}$ of the two electrons. The blue and the red curves correspond to the cases including and excluding the final-state *e-e* repulsion, respectively. From Figs. 2(a)–2(c) one can see that the distinct two-line-shaped structure is always obvious for all three ionization time

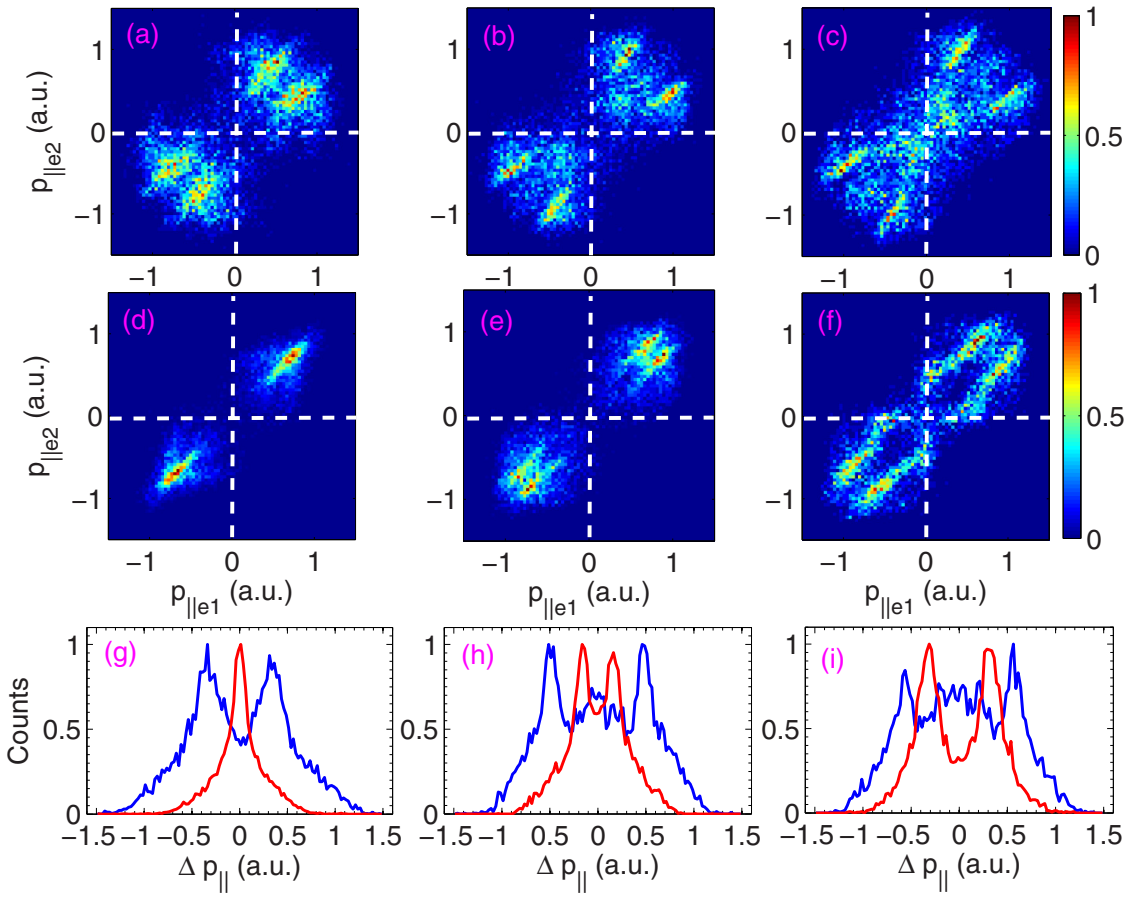

FIG. 3. First row: correlated-electron momentum distributions including final-state *e-e* repulsion. Second row: correlated-electron momentum distributions excluding final-state *e-e* repulsion. Third row: distributions of longitudinal momentum difference $\Delta p_{||}$ of two electrons. The blue and red curves represent the cases including and excluding the final-state *e-e* repulsion. Each column from left to right corresponds to ionization time difference of $[0T, 0.01T]$, $[0.03T, 0.04T]$, and $[0.06T, 0.08T]$, respectively. These time intervals are also marked with shadows in Fig. 2(c).

differences, which is manifested in the form of a double-hump structure in the distributions of longitudinal momentum difference $\Delta p_{||}$ of the two electrons [see the blue curves in Fig. 3(g)–3(i)]. That is to say, there exists always a clear momentum difference between the two electrons. And the momentum difference of the two electrons increases gradually with increasing ionization time difference. Once the final-state *e-e* repulsion is excluded, as shown in Figs. 2(d)–2(f), the results are quite different. For the ionization time difference of $[0T,0.01T]$, as shown in Fig. 2(d), most of NSDI events are located at the diagonal, i.e., the two electrons from NSDI have the same longitudinal momentum. It is easily understood that according to the simple-man model [8,9], the electron final drift momentum obtained from the laser electric field is decided by the ionization time. Thus the two electrons with near-zero ionization time difference obtain the same longitudinal momentum. Further, from Figs. 2(d)–2(f), we can see that the momentum difference of the two electrons increases gradually with increasing ionization time difference. By comparing Figs. 2(a)–2(c) with Figs. 2(d)–2(f), it is obvious that when the final-state *e-e* repulsion is neglected, the momentum difference of the two electrons decreases significantly. This is more clearly shown in Figs. 3(g)–3(i).

When the long-range potential is used for final-state *e-e* interaction, the momentum difference originates from the ionization time difference and the final-state *e-e* repulsion. When the final-state *e-e* repulsion is neglected by replacing the long-range Coulomb repulsion with the short-range Yukawa potential, only the role of the ionization time difference remains. Thus we estimate the contribution of the final-state *e-e* repulsion on the momentum difference of the two electrons by comparing those results from the two cases. The momentum differences originating from the final-state *e-e* repulsion are 0.33 a.u. for $[0T,0.01T]$, 0.30 a.u. for $[0.03T,0.04T]$, and 0.25 a.u. for $[0.06T,0.08T]$, respectively. This indicates that with the ionization time difference increasing, the role of the final-state *e-e* repulsion decreases gradually. This is because for NSDI events with the large ionization time difference when the second electron is ionized, the first electron has moved far away and thus the Coulomb repulsion between the two electrons is relatively small.

Further, we investigate the NSDI of molecules aligned perpendicular to the laser polarization for all CEPs averaged. Different from the parallel molecules, the correlated-electron momentum distribution, as shown in Fig. 4(a), shows clear anticorrelation behavior. To clarify the origin of anticorrelated-

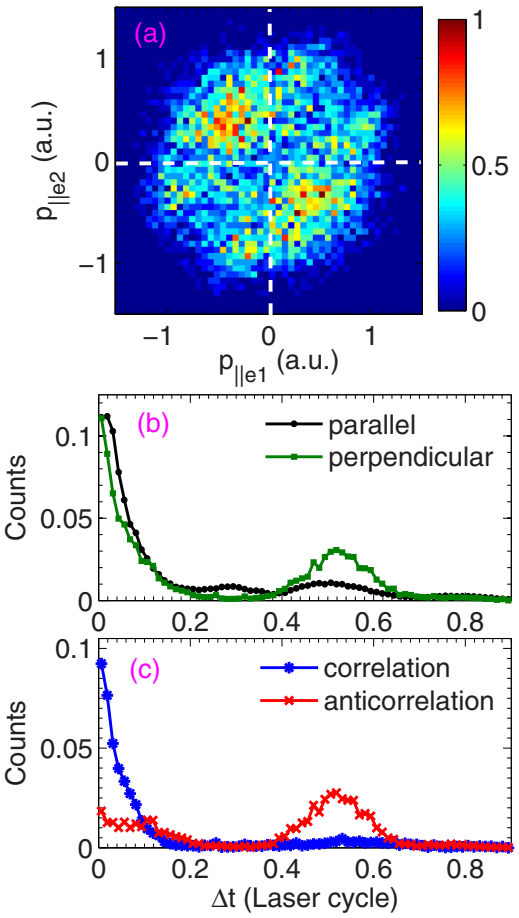

FIG. 4. (a) Correlated-electron momentum distribution for NSDI of molecules aligned perpendicular to the laser polarization by 800 nm, four-cycle linearly polarized laser pulses at the intensity of 1×10^{14} W/cm^2 for all CEPs averaged. (b) Distributions of ionization time difference of two electrons from the doubly excited state. Black curve: parallel alignment case; green curve: perpendicular alignment case. (c) Counts of correlation (blue curve) and anticorrelation (red curve) events as a function of ionization time difference of two electrons for perpendicular molecules. The ensemble size is 4×10^8 for perpendicular molecules.

electron emissions, we trace classical NSDI trajectories. Figure 4(b) shows the distributions of ionization time difference of the two electrons from the doubly excited state for parallel molecules (black curve) and perpendicular molecules (green curve). Obviously, compared to parallel molecules, more NSDI events occur with near $0.5T$ time difference for perpendicular molecules. Moreover, we present counts of correlation (blue curve) and anticorrelation (red curve) events as a function of ionization time difference of the two electrons from the doubly excited state for perpendicular molecules in Fig. 4(c). It clearly shows that for perpendicular molecules the correlation events are mainly located within ionization time difference of $0.2T$. But the anticorrelation events are mainly clustered around ionization time difference of $0.5T$. That is to say, just because ionizations of the two electrons have longer time differences (near $0.5T$) for perpendicular molecules than for parallel molecules, more anticorrelated emissions occur for perpendicular molecules. The longer ionization time difference for perpendicular molecules should be attributed to the higher suppressed potential barrier compared to parallel molecules [40].

IV. CONCLUSION

In conclusion, we have investigated the NSDI of aligned molecules by few-cycle laser pulses at low intensity. Similar to the case of atoms, NSDI of aligned molecules by few-cycle laser pulses at low intensity occurs through a transition doubly excited state induced by recollision. The correlated-electron momentum distribution of parallel molecules exhibits a line-shaped structure parallel to the diagonal. Besides the ionization time difference of two electrons from doubly excited state, the role of the final-state e-e repulsion in the formation of the line-shaped structure is demonstrated. Moreover, for perpendicular molecules by few-cycle laser pulses at low intensity, prominent near half-cycle emission delay between two electrons results in clear anticorrelation behavior.

ACKNOWLEDGMENTS

This work was supported by "Fundamental Research Funds for the Central Universities" under Grant No. XDJK2015C148, SWU114069, and the National Natural Science Foundation of China under Grants No. 11504302, No. 61178011, and No. 61475127.

[1] A. l'Huillier, L. A. Lompre, G. Mainfray, and C. Manus, Phys. Rev. A **27**, 2503 (1983); D. N. Fittinghoff, P. R. Bolton, B. Chang, and K. C. Kulander, Phys. Rev. Lett. **69**, 2642 (1992); B. Walker *et al.*, *ibid.* **73**, 1227 (1994); C. Guo, M. Li, J. P. Nibarger, and G. N. Gibson, Phys. Rev. A **58**, R4271(R) (1998).

[2] A. Becker, R. Dörner, and R. Moshammer, J. Phys. B **38**, S753 (2005).

[3] W. Becker, X. Liu, P. Jo Ho, and J. H. Eberly, Rev. Mod. Phys. **84**, 1011 (2012).

[4] C. Figueira de Morisson Faria and X. Liu, J. Mod. Opt. **58**, 1076 (2011).

[5] A. N. Pfeiffer, C. Cirelli, M. Smolarski, R. Döner, and U. Keller, Nat. Phys. **7**, 428 (2011); A. N. Pfeiffer, C. Cirelli, M. Smolarski, X. Wang, J. H. Eberly, R. Döner, and U. Keller, New J. Phys. **13**, 093008 (2011).

[6] Y. Zhou, C. Huang, Q. Liao, and P. Lu, Phys. Rev. Lett. **109**, 053004 (2012); Y. Zhou, Q. Zhang, C. Huang, and P. Lu, Phys. Rev. A **86**, 043427 (2012); Y. Zhou *et al.*, Opt. Express **20**, 20201 (2012); A. Tong *et al.*, *ibid.* **23**, 15774 (2015).

[7] X. Wang and J. H. Eberly, J. Chem. Phys. **137**, 22A542 (2012); X. Wang, J. Tian, and J. H. Eberly, Phys. Rev. Lett. **110**, 073001 (2013).

[8] P. B. Corkum, Phys. Rev. Lett. **71**, 1994 (1993).

[9] K. J. Schafer, B. Yang, L. F. DiMauro, and K. C. Kulander, Phys. Rev. Lett. **70**, 1599 (1993).

[10] B. Feuerstein, R. Moshammer, D. Fischer, A. Dorn, C. D. Schroter, J. Deipenwisch, J. R. Crespo Lopez-Urrutia, C. Hohr, P. Neumayer, J. Ullrich, H. Rottke, C. Trump, M. Wittmann, G. Korn, and W. Sandner, Phys. Rev. Lett. **87**, 043003 (2001).

[11] B. Eckhardt, J. S. Prauzner-Bechcickib, K. Sachac, and J. Zakrzewski, Chem. Phys. **370**, 168 (2010).

[12] Th. Weber *et al.*, Nature (London) **405**, 658 (2000); R. Moshammer, B. Feuerstein, J. Crespo Lopez-Urrutia, J. Deipenwisch, A. Dorn, D. Fischer, C. Hohr, P. Neumayer, C. D. Schroter, J. Ullrich, H. Rottke, C. Trump, M. Wittmann, G. Korn, and W. Sandner, Phys. Rev. A **65**, 035401 (2002); M. Weckenbrock, D. Zeidler, A. Staudte, T. Weber, M. Schoffler, M. Meckel, S. Kammer, M. Smolarski, O. Jagutzki, V. R. Bhardwaj, D. M. Rayner, D. M. Villeneuve, P. B. Corkum, and R. Dorner, Phys. Rev. Lett. **92**, 213002 (2004).

[13] Y. Zhou *et al.*, Opt. Express **19**, 2301 (2011); Opt. Lett. **36**, 2758 (2011).

[14] M. Lein, E. K. U. Gross, and V. Engel, Phys. Rev. Lett. **85**, 4707 (2000).

[15] L. Zhang, X. Xie, S. Roither, Y. Zhou, P. Lu, D. Kartashov, M. Schöffler, D. Shafir, P. B. Corkum, A. Baltuška, A. Staudte, and M. Kitzler, Phys. Rev. Lett. **112**, 193002 (2014).

[16] X. Sun, M. Li, D. Ye, G. Xin, L. Fu, X. Xie, Y. Deng, C. Wu, J. Liu, Q. Gong, and Y. Liu, Phys. Rev. Lett. **113**, 103001 (2014).

[17] X. L. Hao, J. Chen, W. D. Li, B. Wang, X. Wang, and W. Becker, Phys. Rev. Lett. **112**, 073002 (2014); M. Y. Wu, Y. L. Wang, X. J. Liu, W. D. Li, X. L. Hao, and J. Chen, Phys. Rev. A **87**, 013431 (2013); J. Guo *et al.*, *ibid.* **88**, 023405 (2013).

[18] A. Staudte, C. Ruiz, M. Schoffler, S. Schossler, D. Zeidler, T. Weber, M. Meckel, D. M. Villeneuve, P. B. Corkum, A. Becker, and R. Dorner, Phys. Rev. Lett. **99**, 263002 (2007).

[19] A. Rudenko, V. L. B. deJesus, T. Ergler, K. Zrost, B. Feuerstein, C. D. Schroter, R. Moshammer, and J. Ullrich, Phys. Rev. Lett. **99**, 263003 (2007).

[20] Q. Liao, Y. Zhou, C. Huang, and P. Lu, New J. Phys. **14**, 013001 (2012).

[21] J. S. Parker, B. J. S. Doherty, K. T. Taylor, K. D. Schultz, C. I. Blaga, and L. F. DiMauro, Phys. Rev. Lett. **96**, 133001 (2006).

[22] Y. Liu, S. Tschuch, A. Rudenko, M. Dürr, M. Siegel, U. Morgner, R. Moshammer, and J. Ullrich, Phys. Rev. Lett. **101**, 053001 (2008).

[23] Z. Chen, Y. Liang, and C. D. Lin, Phys. Rev. Lett. **104**, 253201 (2010).

[24] D. F. Ye, X. Liu, and J. Liu, Phys. Rev. Lett. **101**, 233003 (2008).

[25] Y. Zhou, Q. Liao, and P. Lu, Phys. Rev. A **82**, 053402 (2010).

[26] S. L. Haan, Z. S. Smith, K. N. Shomsky, and P. WPlantinga, J. Phys. B **41**, 211002 (2008).

[27] X. Liu, H. Rottke, E. Eremina, W. Sandner, E. Goulielmakis, K. O. Keeffe, M. Lezius, F. Krausz, F. Lindner, M. G. Schatzel, G. G. Paulus, and H. Walther, Phys. Rev. Lett. **93**, 263001 (2004).

[28] Q. Liao *et al.*, J. Phys. B **41**, 125601 (2008); H. Li *et al.*, *ibid.* **42**, 125601 (2009).

[29] C. F. Faria, X. Liu, A. Sanpera, and M. Lewenstein, Phys. Rev. A **70**, 043406 (2004); **86**, 053405 (2012).

[30] Y. Zhou, Q. Liao, Q. Zhang, W. Hong, and P. Lu, Opt. Express **18**, 632 (2010).

[31] C. Ruiz, L. Plaja, L. Roso, and A. Becker, Phys. Rev. Lett. **96**, 053001 (2006).

[32] B. Bergues *et al.*, Nat. Commun. **3**, 813 (2012).

[33] M. Kubel, N. G. Kling, K. J. Betsch, N. Camus, A. Kaldun, U. Kleineberg, I. Ben-Itzhak, R. R. Jones, G. G. Paulus, T. Pfeifer, J. Ullrich, R. Moshammer, M. F. Kling, and B. Bergues, Phys. Rev. A **88**, 023418 (2013).

[34] N. Camus, B. Fischer, M. Kremer, V. Sharma, A. Rudenko, B. Bergues, M. Kubel, N. G. Johnson, M. F. Kling, T. Pfeifer, J. Ullrich, and R. Moshammer, Phys. Rev. Lett. **108**, 073003 (2012).

[35] D. Zeidler, A. Staudte, A. B. Bardon, D. M. Villeneuve, R. Dörner, and P. B. Corkum, Phys. Rev. Lett. **95**, 203003 (2005).

[36] S. L. Haan, L. Breen, A. Karim, and J. H. Eberly, Phys. Rev. Lett. **97**, 103008 (2006).

[37] Phay J. Ho, R. Panfili, S. L. Haan, and J. H. Eberly, Phys. Rev. Lett. **94**, 093002 (2005); S. L. Haan, J. S. Van Dyke, and Z. S. Smith, *ibid.* **101**, 113001 (2008).

[38] Y. Zhou, C. Huang, and P. Lu, Phys. Rev. A **84**, 023405 (2011); C. Huang *et al.*, Opt. Express **21**, 11382 (2013).

[39] F. Mauger, C. Chandre, and T. Uzer, Phys. Rev. Lett. **102**, 173002 (2009); F. Mauger, A. Kamor, C. Chandre, and T. Uzer, *ibid.* **108**, 063001 (2012).

[40] C. Huang, Y. Zhou, A. Tong, Q. Liao, W. Hong, and P. Lu, Opt. Express **19**, 5627 (2011).